

Continuous Column Studies for Water Defluoridation Using Synthesized Magnesium-incorporated Hydroxyapatite Pellets: Experimental and Modeling Studies

Poonam Mondal¹ · Dhiraj Mehta¹ · Virendra Kumar Saharan¹ · Suja George¹

Received: 25 October 2017 / Accepted: 25 January 2018 / Published online: 5 March 2018
© Springer International Publishing AG, part of Springer Nature 2018

Abstract This study presents the synthesis of magnesium-incorporated hydroxyapatite (M-i-HAPa) pellets and evaluation of its defluoridation potential via column studies. Characterization of M-i-HAPa was conducted to analyze the phase composition, bonding patterns, elemental details and microstructural characteristics. An adsorption-regeneration experimental setup was used to study the breakthrough performances and the effect of varying process parameters such as flow rate, bed height, feed fluoride concentration, particle size and particle shape. The experimental studies of varying flow rate and size of particles were evaluated with simulated runs from an adsorption simulator “ADSORB” developed in MATLAB software. The column adsorption capacity was observed to be 1.46 mg/g at feed fluoride concentration of 10 mg/L, flow rate of 1 L/h and bed height of 30 cm. Studies on the column breakthrough performances under different process conditions indicated that bed height of 30 cm with 1–1.5 mm pellets of spherical particle sizes and flow rate of 1 L/h for an initial feed fluoride concentration of 10 mg/L was optimum for efficient column performance. Regeneration of M-i-HAPa pellets was achieved using 0.1 M NaOH solution; however, its capacity was reduced to 40% of its initial capacity after the third cycle. The treated water quality parameters tested after the defluoridation process were found to be under permissible limits as per WHO and BIS guidelines, ensuring the promising nature of M-i-HAPa pellets as a viable adsorbent for defluoridation. A domestic defluoridation unit was also designed which can treat

Highlights

- Synthesis of a novel adsorbent magnesium-incorporated hydroxyapatite (M-i-HAPa) pellets
- Continuous column based defluoridation and regeneration upto four cycles with 0.1 M NaOH
- Domestic Defluoridation unit using M-i-HAPa for treating groundwater of fluoride prone areas
- Calcium and Magnesium content of treated drinking water within the permissible limits.

Electronic supplementary material The online version of this article (<https://doi.org/10.1007/s40710-018-0287-6>) contains supplementary material, which is available to authorized users.

✉ Suja George
sgeorge.chem@mnit.ac.in

¹ Department of Chemical Engineering, Malaviya National Institute of Technology Jaipur, Rajasthan 302017, India

approximately 348 L of fluoride water at a concentration of 10 mg/L using 3 kg of M-i-HAPa pellets with a fluoride uptake capacity of 1.16 mg/g.

Keywords Fluoride · Drinking water · Adsorbent · Column studies · Hydroxyapatite · Magnesium

1 Introduction

Safe drinking water can be said to be the elixir for human life, but in the current scenario millions of people around the globe are not fortunate enough to access it due to presence of various contaminants. One of the chief groundwater contaminant is fluoride, and excess fluoride (>1.0 mg/L) (BIS 2012) in groundwater has been recounted in a number of tropical countries such as India, China, Pakistan, Turkey, Iraq, Afghanistan, Mexico, and Africa (Meenakshi 2006). Fluoride intake in excess may lead to dental and skeletal fluorosis. At the molecular level, many toxicological effects are triggered by fluoride (Mondal and George 2015a).

Defluoridation of water for drinking purposes has been carried out using various techniques such as reverse osmosis, nanofiltration, electrocoagulation and adsorption (Mehta et al. 2017; Mehta et al. 2018; Bhaumik and Mondal 2015). Considerable research has been done on mitigation of fluoride by adsorption mechanism. Conventionally, aluminum-based adsorbents are used for defluoridation due to their high capacity owing to their affinity towards fluoride ions. However, recent studies by George et al. (2009) and George et al. (2010) indicate leaching of aluminum ions into treated water using activated alumina and alum through the Nalgonda process causing adverse health issues since the permissible limit of aluminum ions is very low (0.2 mg/L). Therefore, the focus of this study was to use non-toxic compounds for fluoride removal, such as calcium and magnesium, which have higher permissible limit in drinking water (75 and 30 mg/L, respectively). Most of the adsorbents studied for defluoridation are by using batch process (Mondal and George 2015a; Mehta et al. 2016; Chen et al. 2014; Fan et al. 2003). Moreover, the adsorbents used for batch defluoridation studies are generally in powder form which makes it impractical to use in a continuous system due to operational difficulties, such as high pressure drop and high pumping costs (Mondal and George 2015a). The practical aspects of defluoridation can be visualized only via continuous column studies since the adsorbent capacity can be utilized efficiently, leading to better quality of treated water. Some researchers have studied the defluoridation ability of different adsorbents in continuous column mode. Tor et al. (2009) prepared granular red mud (GRM) and evaluated its potential use to remove fluoride ions from water. The potential of alumina cement granules (ALC) in defluoridating drinking water was studied by Ayoob et al. (2008) by analyzing the effect of various factors affecting its sorption profile.

Fluorosis is a disease characterized by the discoloration and mottling of teeth and weakening of the bones especially caused in people due to continuous intake of high fluoride through drinking water over a prolonged period of time. This condition gets aggravated with calcium deficiency and this disease attacks the calcium containing tissues, especially bones and teeth, in the body due to their high affinity for fluoride ions. This characteristic property of affinity of calcium ions towards fluoride ions was considered in our previous study for selection of synthetic bone material hydroxyapatite ($\text{Ca}_{10}(\text{PO}_4)_6(\text{OH})_2$) for defluoridation of groundwater (Mondal et al. 2016). Presence of magnesium also plays important role in calcium metabolism through its involvement in normal activity of the hormones controlling

calcium utilization. Adequate serum magnesium levels are necessary for proper calcium metabolism since hypomagnesemia can result in hypocalcemia and adequate calcium intake may not ensure proper bone health if magnesium status is abnormal. Magnesium influences both matrix and mineral metabolism in human body, and depletion in magnesium levels adversely affect all stages of skeletal metabolism (Percival 1999). Incorporation of magnesium ions into hydroxyapatite will enhance its defluoridation capacity since magnesium also has very good affinity for fluoride ions. Many researchers have also used magnesium to enhance the fluoride adsorption rate, such as magnesium incorporated bentonite clay and magnesium-amended activated alumina (Thakre et al. 2010; Kamble et al. 2009; Maliyekkal et al. 2008). Therefore, magnesium was incorporated into hydroxyapatite and M-i-HAPa (magnesium incorporated hydroxyapatite) was synthesized for effective fluoride adsorption (Mondal and George 2015b; Mondal et al. 2016) and studies were only focused on batch defluoridation experiments with synthesized powder of M-i-HAPa, a novel adsorbent. Therefore, for facilitating engineering applications, emphasis was given in the present study to convert the powdered M-i-HAPa adsorbent into pellets of suitable size using extrusion and spheronization techniques. Wet-mass extrusion and spheronization is an established technique for producing spherical shaped pellets (Wilson and Rough 2007; Young et al. 2002). Polyvinyl alcohol was selected as a binder due to its chemical stability and nontoxic properties. It can be amended to reduce swelling in water and has ability to form net like arrangement for enclosing active constituents through $-OH$ bond cross-linking via esterification with dicarboxylic acids (Isiklan and Sanli 2005; Chabert et al. 2008).

The present work is focused on pelletizing the adsorbent into suitable size for performing continuous defluoridation studies, and this technique was never being used for the preparation of pellets of M-i-HAPa adsorbent. Verification of experimental data with column simulation studies was also done using MATLAB software. Modeling and simulation process is substantial for its theoretical approach because it entails the system parameters, process characteristics and working conditions in order to deliver almost precise solutions predicting the overall performance of the adsorption process that can be utilized to predict parameters useful in design of adsorber. Field studies were also conducted in this study and a domestic defluoridation unit has been designed to obtain treated water quality which was tested for conforming to WHO and BIS standards.

2 Materials and Methods

2.1 Synthesis of M-I-HAPa and Pellet Preparation

Magnesium incorporated hydroxyapatite ($Ca_{10-p}Mg_p(PO_4)_6$) was synthesized via chemical precipitation process. All chemicals used were of analytical reagent (AR) grade supplied by Merck Pvt. Limited, India. The process of adsorbent synthesis and batch studies to estimate the defluoridation capacity of M-i-HAPa, including its adsorption equilibria and kinetic parameters, have been reported in our previous work (Mondal et al. 2016). The synthesis route is diagrammatically represented in Fig. 1a.

The synthesized magnesium incorporated hydroxyapatite powder was further used for preparation of pellets in order to be used for column studies. Polyvinyl alcohol (PVA) was dissolved in double distilled water at 10 wt% concentration possessing a viscosity of 25–32 cP at 90 °C in a water bath, and thereafter, cross-linked with malonic acid (5 wt% of PVA) at 95 ± 2 °C for 5 h. The M-i-HAPa adsorbent in powder form and cross-linked PVA acquired as a binder were mixed

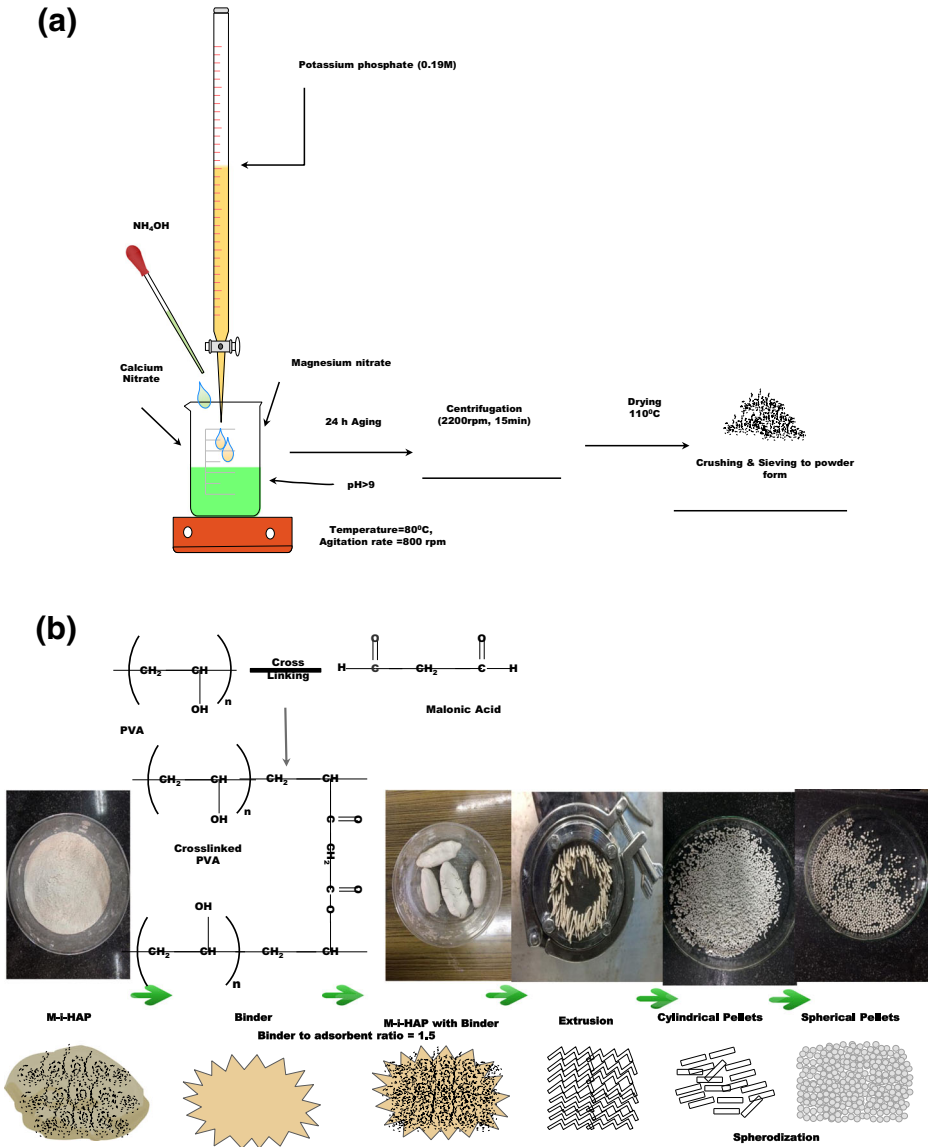


Fig. 1 a M-i-HAPa Synthesis b Pellets Preparation using E-S technique

thoroughly and granulated to cylinder-shaped granules of various diameters (2 mm to 3 mm) using an extruder (PRISM make). The extruder speed was kept at 60 rpm. These granules thus obtained were manually cut into small bars of 3 to 5 mm in length. The powdered M-i-HAPa was granulated with a sieve of 1 mm using an oscillating granulator (PRISM make).

The extruded material was fed into a spheronizer for making spherical shaped pellets by the action of a horizontal rotating friction plate. The spheronizer was fitted with a chequered plate, operated at a speed of 750 to 850 rpm and compressed air was provided at a pressure of 2 kg/cm² for 2–3 min. The spherical pellets thus obtained were dried at 70 ± 2 °C for 4 h before

being used in column studies. Zhao et al. (2012) reported that exposure to temperature as high as 130 °C can destroy PVA structure, therefore, 70 °C was chosen as drying temperature for pellets. A schematic diagram of the whole process is illustrated in Fig. 1b.

2.2 Characterization of M-I-HAPa Pellets

The bonding patterns and functional groups in M-i-HAPa pellets were examined using a Perkin Elmer Fourier transform infrared spectrophotometer (FTIR) (UTR TWO) in the range of 450–4000 cm^{-1} with a resolution of 4 cm^{-1} . X-ray diffraction patterns were recorded on PANalytical X'pert powder X-ray diffractometer (Cu $K\alpha = 1.5406 \text{ \AA}$ radiation source) operating at 40 kV and 30 mA. The samples were scanned for 2θ range from 10° to 80° with step size of 0.15° and scan step time of 3 s. Identification of phases in the samples were carried out by comparing the diffraction data with standards of JCPDS database using PANalytical X'PertHighScore software. The surface morphology and microstructure of M-i-HAPa pellets were visualized by means of scanning electron microscopy (Nova Nano SEM 450). The adsorbent sample was coated with a thin film of platinum using JEOL/JFC1600 Auto fine coater (30 to 90 s as needed at current of 50 mA at vacuum) to reduce the charging of the sample so that conductivity of sample can be increased. Concurrently, for analyzing the elemental compositions of the sample, energy dispersive spectroscopy (EDS) was employed (Xflash 6TI30 Bruker).

M-i-HAPa pellets were also analyzed before fluoride adsorption, after fluoride adsorption and after regeneration using X-ray photoelectron spectroscopy (XPS; Omicron nanotechnology) with Mg $K\alpha$ X-ray source (1253.6 eV of photons) to determine the Ca, O, Mg, F and P contents on the adsorbent surface. The surface area and pore size distribution of the pellet were calculated from the corresponding nitrogen adsorption-desorption isotherm at 77.57 K using a Micrometrics ASAP analyzer 2010. The specific surface area was calculated using the BET isotherms, and the pore size distribution was determined by using the density functional theory (DFT).

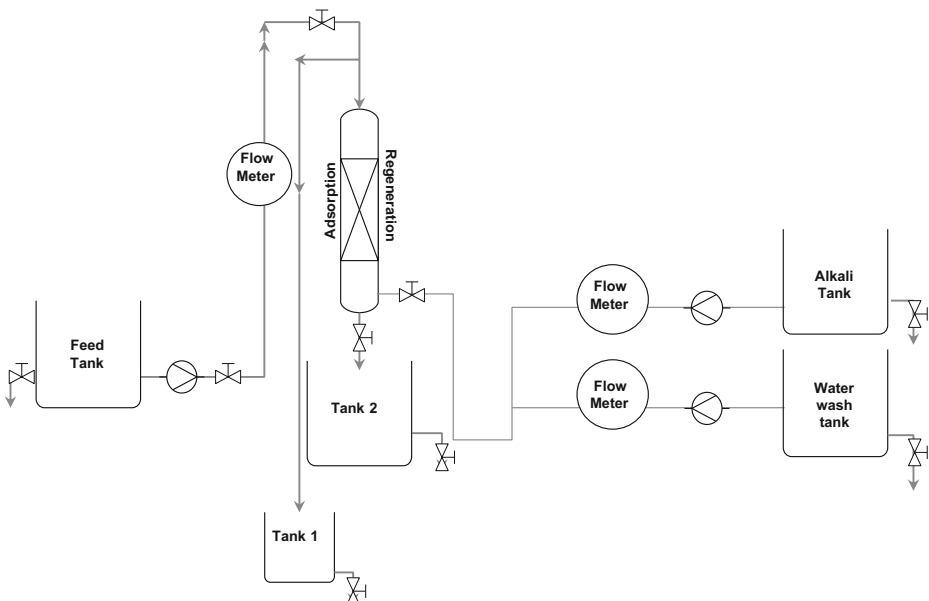


Fig. 2 Line diagram for the experimental setup

2.3 Continuous Fluoride Adsorption and Regeneration Experiments

The schematic diagram of adsorption-regeneration column setup used for this study is presented in Fig. 2. The entire setup was made of stainless steel (SS304). The column length was 50 cm and internal diameter was 5 cm. Feed solution was pumped from a stainless-steel tank of 20 L through a packed column with a magnetic drive pump (Promivac, Daryaganj, New Delhi) and the flow rate was controlled through a flowmeter (Eureka, Maharashtra, India). For regeneration experiments, the eluent was pumped from another tank (Alkali tank) in upflow mode. Tank 1, shown in Fig. 2, was used for storing the overflow solution and Tank 2 was used for collecting the treated water.

Before starting column experiments, double distilled water (stored in a 20 L tank) was run through the column for 2 h, so that equilibrium was established between fluid flow distribution, M-i-HAPa pellets and water. Fluoride solution with known initial concentration was fed from the top of the column with different bed heights at predetermined flow rates continuously. Treated water samples were collected from the bottom of the column at definite time intervals and analyzed for obtaining breakthrough curves.

For column regeneration, when the residual fluoride concentration in outlet became almost constant and equal to the inlet concentration, it was assumed that the M-i-HAPa adsorbent pores were saturated with fluoride ions. The desorption experiments in column studies were carried out using the upflow mode, because a better and faster regeneration rate was observed via this mode due to good contact between the exhausted bed and regenerant solution. The exhausted column was regenerated using the eluent solution of 0.1 M NaOH which had a high regeneration capacity (Mondal et al. 2016) at a flow rate of 1 L/h in upflow mode until maximum amount of the adsorbed fluoride was recovered. The adsorbent bed was restored by washing with double distilled water for approximately 4 h in the aforesaid upflow mode with the same flowrate until the pH of the water collected from the outlet was neutral (7.0 ± 0.1). The bed was then reused and its performance was assessed.

The residual fluoride concentration was analyzed using an ion selective electrode (Orion Versa Star, Thermoscientific, USA). Calibrations were done using fluoride standards and the electrode slope was -59.16 ± 3 mV/decade at 25 ± 0.5 °C. Standard fluoride solutions with fluoride concentrations ranging from 0.5 to 10 mg/L were prepared from standard stock solution of 1000 mg/L. For de-complexation of complexes and avoiding interference with the electrode performance, TISAB-II solution was added at 1:1 proportion to 10 mL sample solution. The column experiments were performed at room temperature (about 30 °C) and no adjustments regarding pH was required. The quantity of fluoride adsorbed was determined by the area under the breakthrough curve for a known fluoride feed concentration using the following equation:

$$q_b = \int_0^{V_b} \frac{C_0 - C_t}{M} dv \quad (1)$$

where q_b is the adsorption capacity up to breakthrough (mg/g), C_0 is the initial concentration of fluoride (mg/L), C_t is the concentration of fluoride at time t (mg/L), M is the mass of adsorbent (g), and V_b is the volume treated up to breakthrough point (L). The total dissolved solids (TDS) and electrical conductivity of treated water was determined using conductivity electrode of ion meter, while turbidity present in the aqueous solution was measured with a turbidity meter (NT4000, Spectra Lab). The calcium concentration, magnesium concentration, total hardness, total alkalinity, and phosphorus concentration of solution were estimated using APHA standard procedures (APHA 2012).

2.4 Column Simulation Studies for Breakthrough Performance

The theoretical model used for predicting fixed bed column adsorption dynamics consisted of mass and energy balance equations, considering external film diffusion followed by internal pore diffusion of fluoride ions on to the adsorbent surface from the bulk medium. An adsorption simulator “ADSORB” was developed in MATLAB® R2014 software incorporating the model equations and predicted the column breakthrough curves with varying process parameters such as flow rate, initial fluoride concentration, bed height etc. The model equations representing the adsorption phenomena within the 3D grid column, basic assumptions, method of numerical solution, input parameters and working algorithm of the simulator are detailed in *Annexure* which is provided as *supplementary material*. The various input values of the parameters to the simulator “ADSORB” are given in Table 1. The dimensionless system parameters were described within the simulator and estimated from the input values. The adsorption simulator “ADSORB” predicted the breakthrough performance of the adsorption bed with varying process parameters such as flow rate, particle size, bed height etc.

3 Results and Discussion

3.1 Characterization of M-I-HAPa Pellets

Various techniques, such as FTIR, XRD, SEM and XPS studies, were used to characterize the M-i-HAPa pellets. BET surface area, pore-volume and pore diameter was also determined for M-i-HAPa pellets.

3.1.1 FTIR Studies

The FTIR spectra of the M-i-HAPa pellets before fluoride adsorption, after fluoride adsorption and after regeneration are presented in Fig. 3. The bands present at 3420 cm^{-1} and 633 cm^{-1} represented the characteristic stretching vibration modes of the -OH group. The peaks observed

Table 1 Input parameters for simulator “ADSORB”

Parameters	Range of values
Radius of adsorbent, m	Varied (0.0005, 0.00075, 0.001)
Bed porosity	0.63
Particle porosity	0.37
Flow rate, m/s	Varied (0.141×10^{-3} , 0.212×10^{-3} , 0.283×10^{-3})
Length of bed, m	0.3
Diameter of bed, m	0.05
Initial concentration, mg/L	10
Solid phase adsorbate concentration, mg/g	1.1
Mass transfer coefficient, m/s	9.5×10^{-11}
Heat of adsorption, J/mol	38.13×10^3
Density of adsorbent, kg/m ³	280
Specific heat of liquid, J/kg.K	4200
Inlet temperature, K	298
Axial mass dispersion coefficient, m ² /s	10^{-5}
Axial heat dispersion coefficient, J/m s K	0.688

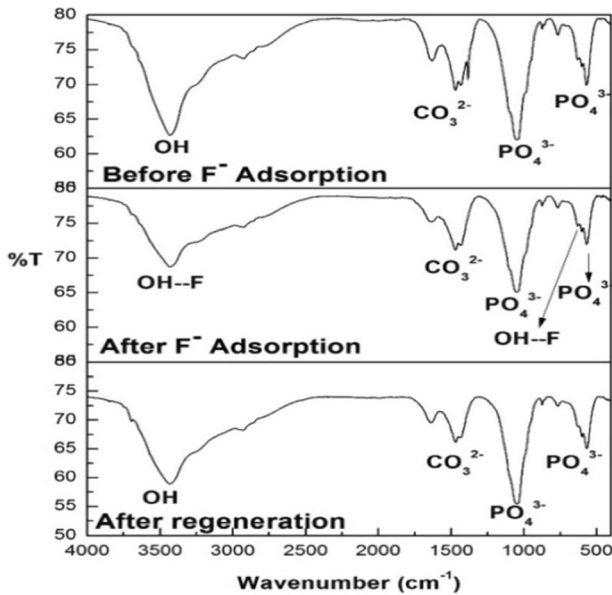


Fig. 3 FTIR spectra of M-i-HAPa pellets

around 1465 cm^{-1} indicated the incorporation of CO_3^{2-} ions in the OH^- sites, because when the reaction conditions were alkaline some OH^- ions from the solution reacted with the atmospheric CO_2 present. The bands for PO_4^{3-} appeared around 1045 cm^{-1} and 565 cm^{-1} corresponding to the characteristic phosphate peaks in apatite. The adsorption capacity of an adsorbent depends on chemical reactivity of functional groups at the adsorbent surface (Senthil Kumar et al. 2010). The FTIR spectra obtained after adsorption of fluoride displayed a significant decrease in intensity of OH^- peaks due to formation of OH-F bonds, which indicated that hydroxyl ions in the adsorbent were replaced by fluoride ions in the adsorption process.

3.1.2 XRD Studies

The XRD patterns of M-i-HAPa pellets before fluoride adsorption (M-i-HAPa pellets), after fluoride adsorption (M-i-HAPa-F pellets) and after regeneration (M-i-HAPa-R pellets) are shown in Fig. 4. The peaks obtained before fluoride adsorption can be indexed to hydroxyapatite and magnesium oxide with JCPDS card numbers 09-0432 and 89-4248, respectively. The pattern obtained after fluoride adsorption revealed the formation of hydroxyfluoroapatite, fluoroapatite and magnesium fluoride corresponding to JCPDS card numbers 034-0010, 034-0011 and 01-1196. This showed that the hydroxyapatite peaks were replaced by hydroxyfluoroapatite and fluoroapatite while the magnesium oxide peak was replaced by magnesium fluoride. After regeneration of M-i-HAPa pellets, the XRD pattern obtained was similar to the one before adsorption of fluoride. The crystallite size calculated as per Scherer equation is 48.7 nm.

3.1.3 SEM Studies

Scanning electron micrographs (SEM) for M-i-HAPa pellets before fluoride adsorption, after fluoride adsorption and after regeneration taken at 2000X magnification are given in Fig. 5. The

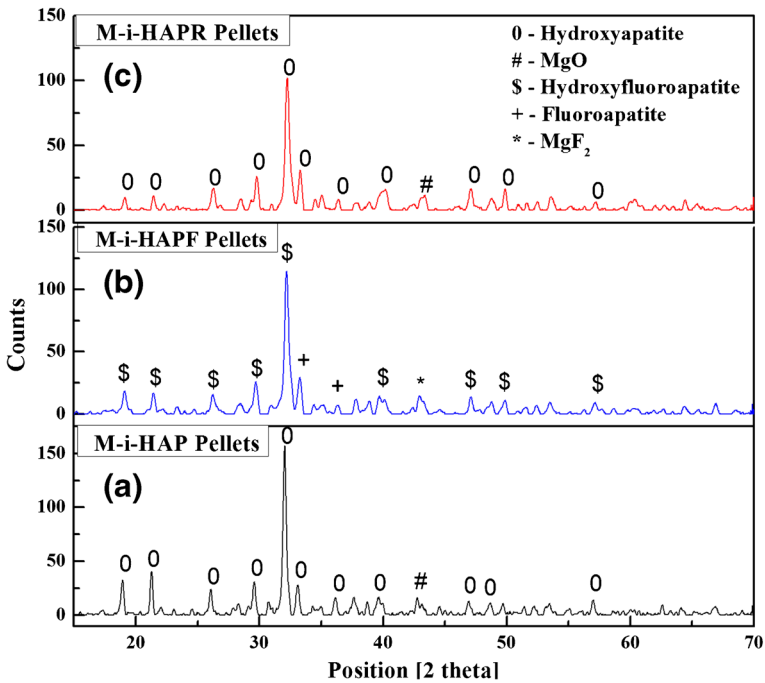


Fig. 4 XRD pattern of M-i-HAPa pellets (a) Fresh pellets (b) After fluoride adsorption (c) After regeneration

fresh pellets showed extremely rough surface with number of pores on the surface which may be used for capturing fluoride ions from the solution (Fig. 5a). For a better glimpse on the surface

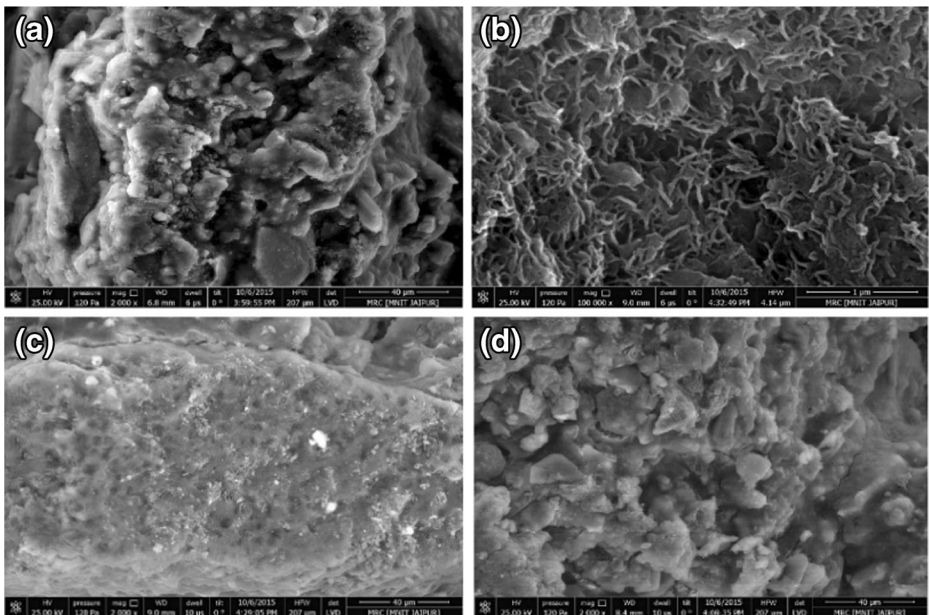


Fig. 5 SEM of M-i-HAPa pellets (a) Before adsorption (2000X magnification) (b) Before adsorption (100,000X magnification) (c) After adsorption (2000X magnification) (d) After regeneration (2000X magnification)

morphology of the unused adsorbent SEM image at 100000X magnification is presented in Fig. 5b, which exhibited the porous nature of the adsorbent. Micrographs of the fluoride loaded M-i-HAPa pellets showed a distinct change in the morphology as compared to micrograph obtained before adsorption indicating complete adherence of the fluoride ions onto the surface and pores, as observed in Fig. 5c. Post regeneration, the surface of the pellets again displayed a porous texture signifying the removal of fluoride from pores, as given in Fig. 5d, which means that the regenerated adsorbent may again be used for defluoridation experiments. However, the pellet surface showed reduced number of pores as compared to the unused adsorbent which pointed to the fact that after each cycle of regeneration, the adsorbent would lose some of its adsorption capacity. The specific surface area of M-i-HAPa pellets was found to be 21.22 m²/g, while the pore volume and pore diameter was observed to be 0.096 cm³/g and 181.59 Å, respectively.

3.2 Experimental Breakthrough Curves

Breakthrough curves were obtained from continuous adsorption experiments and the performances were evaluated by varying parameters such as shape and size of particles, flow rate, feed fluoride concentration and bed height. The column breakthrough curves were obtained by plotting the fluoride concentration (C_e/C_0) against time (t), where C_e is the concentration of fluoride at equilibrium (mg/L), C_0 is the initial concentration (mg/L). The breakthrough concentration (C_b) in this study was taken as 1 mg/L, i.e., the permissible limit for fluoride in water as determined by Indian drinking water specification (2012) and the breakthrough point or time (t_b) is the time at which the effluent concentration (C_e) from the column is equal to C_b . The adsorbent mass for 5, 10 and 30 cm bed heights were 14, 27 and 80 g, respectively, and the density of the adsorbent was 280 kg/m³. The effects of parameters such as shape, size, flow rate, bed height and initial fluoride concentration on the breakthrough performance are discussed below:

3.2.1 Effect of Shape of Pellets

Cylindrical shaped pellets of 0.5–1 mm in length, 0.5–1 mm in diameter (mean equivalent diameter = 1.12 mm) and spherical shaped pellets of 1 to 1.5 mm in diameter were tested for fluoride removal in the continuous column adsorption system. The flow rate, bed height and feed fluoride concentration were kept constant at 1 L/h, 30 cm and 10 mg/L, respectively. The breakthrough curves obtained showed that spherical pellets were more efficient of removing fluoride ions from the solution as compared to cylindrical shaped pellets. The breakthrough time (t_b) and exhaustion time (t_{EX}) of cylindrical shaped pellets were 3 h and 6.5 h, respectively, while that for spherical pellets were 13 h and 16 h, respectively, as seen in Fig. 6a. Faster breakpoint was achieved with cylindrical pellets and the adsorption capacities were also less than those of spherical pellets. The equivalent diameter of cylindrical particles (1.12 mm) being lower than those of the spherical particles (1.25 mm) offered lower adsorption capacity. This might be due to discrepancies in flow patterns like channeling within the cylindrical pellet bed responsible for decrease in adsorption capacity. The adsorption capacity up to breakthrough (q_b) and exhaustion (q_{EX}) for spherical pellets were 1.46 mg/g and 1.8 mg/g, respectively, while the respective values corresponding to cylindrical pellets were 0.34 mg/g and 0.73 mg/g. The delayed breakthrough observed for spherical pellets is because of the higher surface area offered due to their structure which led to higher adsorption capacity. Therefore, spherical particles were used for further experimentations.

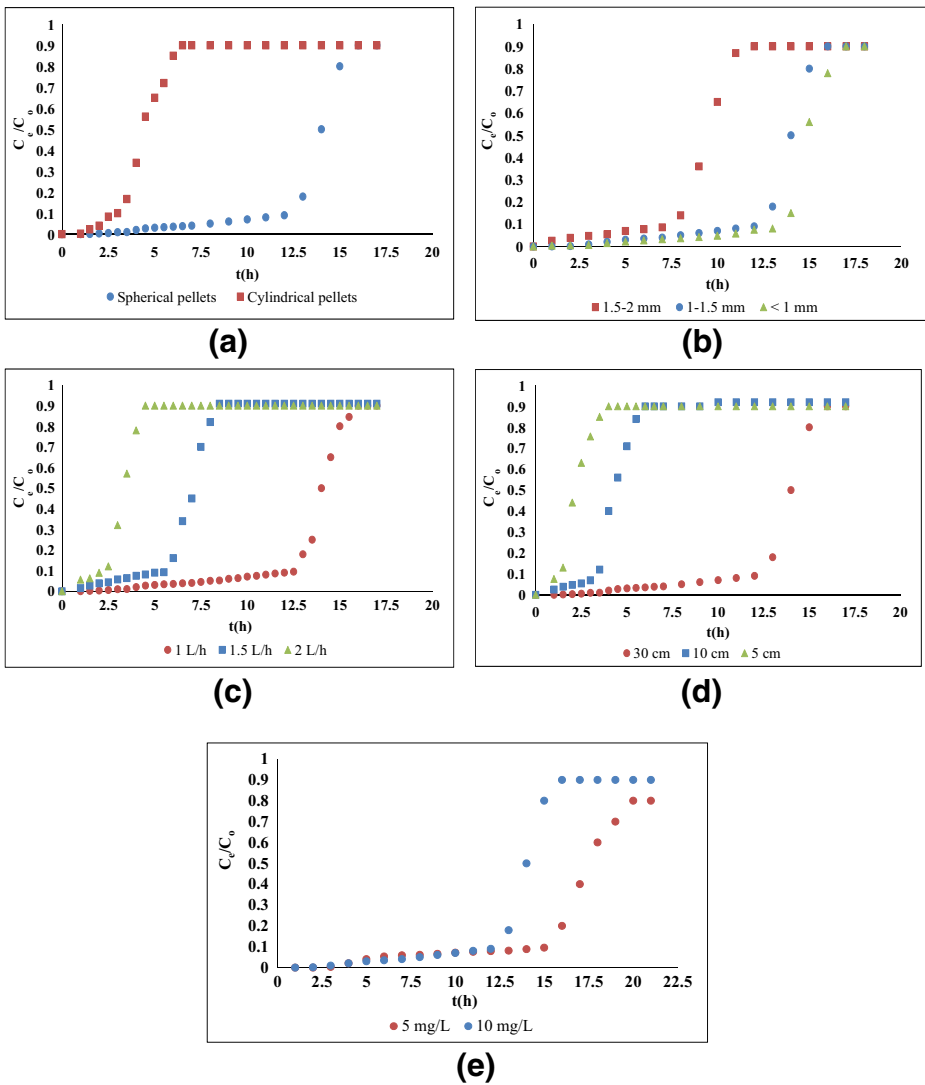


Fig. 6 Effect of varying parameters influencing column adsorption behavior (a) Shapes of pellets (b) particle size (c) flow rate (d) bed height (e) feed fluoride concentration

3.2.2 Effect of Size of Spherical Pellets

Adsorbent pellets of three different sizes, i.e., <1 mm, 1–1.5 mm (average size 1.25 mm) and 1.5–2 mm (average size: 1.75 mm) were used in column studies for obtaining the breakthrough curves and estimating the adsorption capacity, while other operational parameters such as bed height, flow rate and feed fluoride concentration were kept constant at 30 cm, 1 L/h and 10 mg/L respectively. As seen from Fig. 6b, the breakthrough time (t_b) and throughput volume up to exhaustion (V_{EX}) increased with decreasing particle size, as listed in Table 2. The fluoride uptake capacity up to breakpoint (q_b) for particle sizes of <1 mm, 1–1.5 mm and 1.5–2 mm particle sizes were observed as 1.57, 1.46 and 0.9 mg/g, respectively. Clearly, smaller particle

Table 2 Experimental F- adsorption data on M-i-HAPa pellets in column system for different process conditions

Parameters	Z (cm)			F (L/h)			Particle size (mm)			C ₀ (mg/L)	
	5	10	30	1	1.5	2	<1	1–1.5	1.5–2	5	10
t _b (h)	1.5	3.5	13	13	6	2.5	14	13	8	16	13
t _{EX} (h)	4	6	16	16	8.5	4.5	17	16	12	20	16
V _b (L)	1.5	3.5	13	13	9	5	14	13	8	20	13
V _{EX} (L)	4	6	16	16	12.75	9	17	16	12	20	16
q _b (mg/g)	0.96	1.16	1.46	1.46	1.01	0.56	1.57	1.46	0.9	0.8	1.46
q _{EX} (mg/g)	2.5	2	1.8	1.8	1.43	1.01	1.91	1.8	1.35	1.0	1.8
EBCT (h)	0.098	0.196	0.588	0.588	0.392	0.294	0.588	0.588	0.588	0.588	0.588

size of pellets delayed the breakpoint and caused increase in adsorption. Better adsorption with smaller particle sizes may be attributed to their large surface areas per unit volume of column which reduced the equilibrium time. With large particle sizes, some of the interior pores were not accessible whereas in small size particles more pores were accessible and diffusion was faster. The particles having size <1 mm showed best fluoride removal capacity but extremely small sizes led to clogging of the mesh present at the bottom of the column, and moreover, some of the adsorbent leached into treated water. On analyzing these results, 1–1.5 mm particle size having highest adsorption capacity was chosen for further experiments.

3.2.3 Effect of Flow Rate

Column adsorption experiments with varied flow rate were conducted at 1, 1.5 and 2 L/h, with the initial fluoride concentrations of 10 mg/L and bed height of 30 cm. Fig. 6c depicts the effect of flow rate on the breakthrough curve at these operating conditions, which indicated that the uptake of fluoride ions onto M-i-HAPa pellets decreased when the flow rate across the bed increased. This is due to the low residence time provided in the column for the adsorption equilibrium to occur at that particular flow rate which caused the solute to elute early from the column, i.e., before equilibrium was achieved. The adsorption capacity for flow rates of 1, 1.5 and 2 L/h was found to be 1.46, 1.01 and 0.56 mg/g, respectively, as determined from the area under the curve, as shown in Fig. 6c. The M-i-HAPa pellets were found to be exhausted at 16, 10 and 4.5 h when the flow rates were 1, 1.5 and 2 L/h, respectively. At these flow rates, the respective empty bed contact times (EBCT) were observed to be 0.588 h, 0.392 h and 0.294 h, i.e., 35.28, 23.62 and 17.64 min, respectively. The EBCT is used to represent the length of time a stream of water is in contact with the adsorbent media. It was noted that the throughput volume also increased with a higher EBCT which means with increase in EBCT, the fluoride ions had more time to contact with the adsorbent resulting in higher removal of fluoride ions in the adsorption column.

3.2.4 Effect of Bed Height

Feed fluoride solution with 10 mg/L concentration was introduced into the adsorption column with 1 L/h flow rate in order to observe the effect of bed height on breakthrough curves. The breakthrough curves for fluoride adsorption on M-i-HAPa pellets at different bed heights of 5, 10 and 30 cm are shown in Fig. 6d. It is evident from Table 2 that the exhaustion time and volume of treated fluoride solution

increased with increasing bed height due to more contact time available for adsorption. On the contrary, the breakthrough curve appeared steeper when the bed height was less indicating faster exhaustion of the adsorbent bed or mass transfer zone available for adsorption. When the bed height was increased from 5 to 30 cm, the throughput volume of water up to breakthrough point (V_b) and exhaustion point (V_{EX}) varied between 1.5 to 13 L and 4 to 16 L, respectively. The fluoride uptake capacities (q_b) at 5, 10 and 30 cm bed height were observed to be 0.96, 1.16 and 1.46 mg/g. The higher fluoride uptake capacity with increase in bed depth was because of larger mass transfer zone available for adsorption with higher surface area of the adsorbent providing more number of binding sites to fluoride ions in solution. From Table 2, the increase in breakthrough time (t_b) is evident with increase in bed height, which shows delayed ' t_b ' points towards higher bed adsorption capacity.

3.2.5 Effect of Initial Fluoride Concentration

Experiments were conducted in column mode with two feed fluoride concentration viz., 5 and 10 mg/L to determine the effect of solute concentration on breakthrough performances while parameters such as bed height and flow rate were kept at 30 cm and 1 L/h (16 mL/min), respectively. It can be seen from Fig. 6e that with increase in fluoride concentration the breakthrough time decreased as the binding sites got quickly exhausted. The breakthrough time was 13 h at 10 mg/L feed fluoride concentration while it was 16 h at 5 mg/L. The fluoride adsorption capacity (q_b) and the total fluoride adsorbed up to exhaustion point (q_{EX}) were also found to increase with increase in feed fluoride concentration. The adsorption capacities of M-i-HAPa pellets at breakpoint and at exhaustion point were observed to increase from 0.8 to 1.46 mg/g and 1 to 1.8 mg/g, respectively, with increase in fluoride concentration from 5 to 10 mg/L. The increase in inlet fluoride concentration increased the driving force for mass transfer, which in turn decreased the length of the adsorption zone (δ). It was also noticed that a rise in the feed fluoride concentration decreased the volume treated before the bed got exhausted as determined in Table 2. This also indicates that as the inlet feed concentration is decreased, the rate of exhaustion of the pellets is decreased. The exhaustion time for the M-i-HAPa pellets was reduced from 20 to 16 h when the fluoride ion concentration was increased from 5 to 10 mg/L (Fig. 6e, Table 2). On analyzing the breakthrough curves (Fig. 6) and the experimental F^- adsorption data for different process conditions (Table 2), it was observed that bed height of 30 cm with 1–1.5 mm pellets of spherical particle sizes and flow rate of 1 L/h and feed fluoride concentration of 10 mg/L were optimum for efficient column performance.

Table 3 Fluoride removal capacity of few adsorbents in comparison with M-i-HAPa pellets

Adsorbent	Fluoride removal capacity (mg/g)	Reference
Manganese dioxide-coated activated alumina	1.22	Tripathy and Raichur 2008
Nano sized synthetic HAP	0.489	Jimenez-Reyes and Solache-Rios 2010
Modified immobilized activated alumina	0.76	Rafique et al. 2012
Laterite	0.85	Sarkar et al. 2006
Calcite	0.39	Fan et al. 2003
M-i-HAPa pellets	1.46	Present study

Table 3 shows a comparison between the fluoride removal capacity of M-i-HAPa pellets and adsorbents such as manganese dioxide coated activated alumina, nano-sized HAP, modified alumina, laterite, calcite etc., which had been previously reported by various researchers. It is observed that fluoride removal capacity of M-i-HAPa pellets is higher as compared to many adsorbents reported in the literature.

3.3 Column Simulation Studies

The experimental breakthrough curves obtained by varying flow rate and size of particles were compared for convergence with simulated curves obtained from the adsorption simulator “ADSORB” (see [supplementary material](#) for details) developed in MATLAB software, and are depicted in Figs. 7 and 8. It is observed that the initial part of breakthrough curve fitted extremely well with the simulated data and little deviation is seen in the latter part of the curves (Figs. 7 and 8). Experimentally, C_e/C_0 was obtained up to 0.9, but through the simulated data this ratio was 0.8. The breakthrough time as per simulated curves for 1, 1.5 and 2 L/h was 13.5, 6 and 3 h, respectively, while the same values corresponding to experimental curves was 13, 6 and 2.5 h, respectively. A comparison of the simulated breakthrough curves for all flow rates of 1, 1.5, 2, 4 and 6 L/h is presented in Fig. 8d. In case of the higher flow rates 4 L/h and 6 L/h, as observed in Fig. 8d, the breakthrough time reached faster, which indicates that the adsorption bed will not be sufficiently utilized. Lower flow rate of 1 L/h is found to be more suitable with a longer breakthrough time and higher adsorption capacity than higher flow rates.

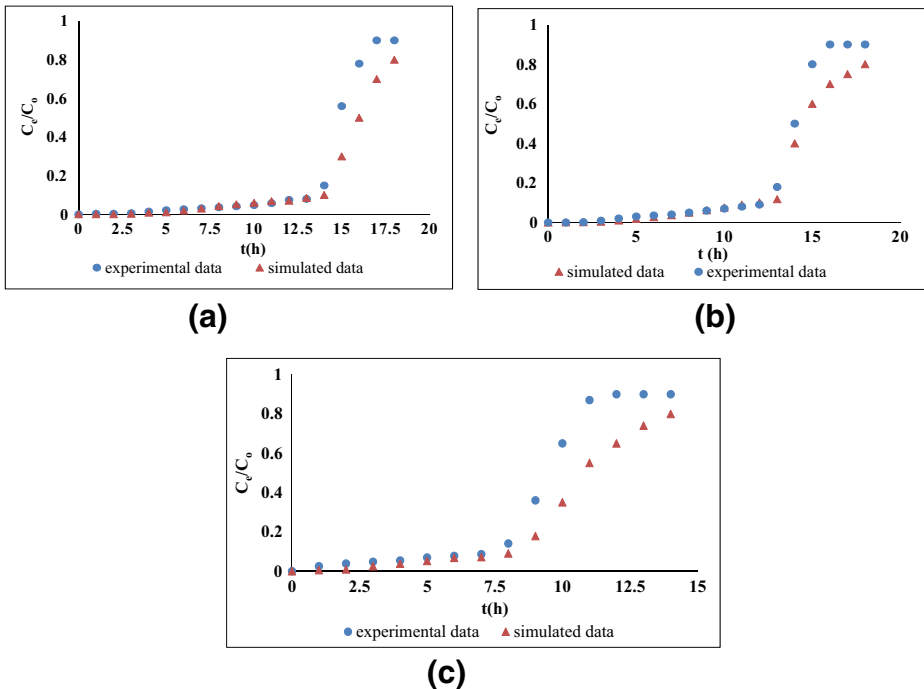


Fig. 7 Breakthrough curves for varying particle sizes (a) size <1 mm (b) size 1–1.5 mm (c) size 1.5–2 mm

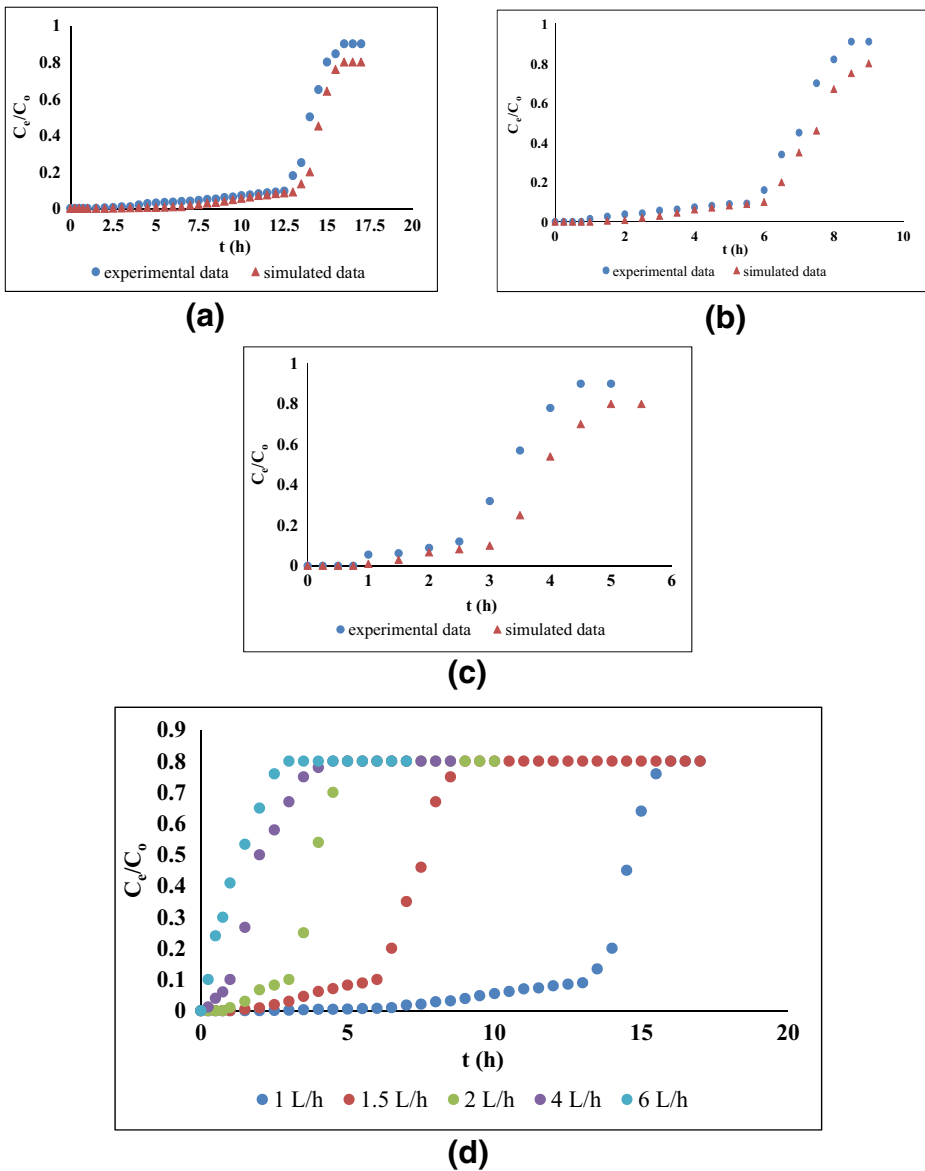


Fig. 8 Breakthrough curves for varying flow rates (a) 1 L/h (b) 1.5 L/h (c) 2 L/h (d) Simulated curves for five different flow rates

3.3.1 Column Design Parameters

The part of the adsorbent bed between C_{EX} (exhaustion concentration in mg/L) and C_b (breakthrough concentration in mg/L) in the breakthrough curve is termed as the primary adsorption zone (PAZ). The breakthrough curves were used to calculate the values of column design parameters such as t_x which is the time to establish primary adsorption zone (h), t_f is the time for formation of primary adsorption zone (h), t_z is the time for movement of primary adsorption zone (h) down the

column, δ is the length of primary adsorption zone, f is the fractional capacity of M-i-HAPa pellets in the adsorption zone, %S is the percentage saturation in column and H_{UNB} is the height of unused bed. The time required for the PAZ to establish and move out of the column was calculated from Eq. (2) (Ghosh et al. 2015; Kundu and Gupta 2005):

$$t_x = \frac{V_{EX}}{F} \tag{2}$$

where t_x is the time for the primary adsorption zone to establish and move out of the column (h), V_{EX} is the volume of liquid treated up to the exhaustion point (L) and F is the flow rate (L/h). The time t_z , defined as the time needed for the movement of adsorption zone down its own length in the column (h), was computed by Eq. (3):

$$t_z = \frac{V_{EX} - V_b}{F} \tag{3}$$

where V_b is the volume treated up to breakthrough point (L). For a bed depth ‘Z’ of M-i-HAPa pellets, the depth and time ratios is given by Eq. (4):

$$\frac{\delta}{Z} = \frac{t_z}{t_x - t_f} \tag{4}$$

where δ is the length of primary adsorption zone (cm), and Z is the bed height (cm). The fractional capacity of the pellets defined as ‘ f ’ in the adsorption zone was computed using Eq. (5):

$$f = \frac{\int_{V_b}^{V_{EX}} (C_0 - C_t) dv}{C_0(V_{EX} - V_b)} \tag{5}$$

where C_0 is the initial concentration (mg/L), C_t is the concentration of fluoride at any time t (mg/L). The term t_f defined as the time for the formation of primary adsorption zone PAZ (h) was estimated using Eq. (6):

$$t_f = (1-f)\delta \tag{6}$$

The percent saturation (%S) of the column was determined using Eq. (7):

$$\%S = \left[1 + \frac{\delta(f-1)}{Z} \right] \times 100 \tag{7}$$

Table 4 Column design parameters

Parameters	Z (cm)			F (L/h)			C ₀ (mg/L)	
	5	10	30	1	1.5	2	5	10
t_x (h)	4	6	16	16	8.5	4.5	20	16
t_z (h)	2.5	2.5	3	3	2.5	2	4	3
t_f (h)	1.37	1.4	1.6	1.6	1.52	1.25	1.8	1.6
δ (cm)	4.77	5.43	6.24	6.24	10.71	18.46	6.59	6.24
f	0.45	0.44	0.467	0.467	0.391	0.375	0.5	0.467
%S	48.3	69.59	88.91	88.91	78.25	61.54	90.1	88.91
H_{UNB} (cm)	3.12	4.16	5.62	5.62	8.82	13.32	6	5.62

The length of unused bed in a column system was calculated using Eq. (8):

$$H_{UNB} = \frac{Z}{t_{EX}} (t_{EX} - t_b) \tag{8}$$

where H_{UNB} is the height of unused bed (cm), t_b is the breakthrough time (h) and t_{EX} is the exhaustion time (h). The estimated values of column design parameters are presented in Table 4. The time required for the formation of the primary adsorption zone was noticed to decrease with decrease in bed height, increase in flow rate and feed fluoride concentrations expected. The higher the bed length, the more time it takes to form the primary adsorption zone. Similarly, with decrease in flow rate, the contact time necessary for formation of the zone also reduces. It was observed that the length of the adsorption zone of column increased as the flow rate and bed height increased. However, the percent saturation for column increased with increasing bed height and decreased with increasing flow rate. On the other hand, the value of fractional capacity of column at breakthrough point decreased in general with rise in flow rate, feed fluoride concentration and decrease in bed height. As the flow rate was elevated, the value of depth of adsorption zone δ increased and the %S decreased since the adsorption zone travelled faster. However, for bed height of 5 cm, 10 cm and fluoride concentration of 5 mg/L, 10 mg/L, the ‘f’ value was approximately the same in this study. Furthermore, owing to the greater degree of freedom of the fluoride ions over the adsorbent pellet surface, the adsorption zone was found to decrease slightly with increase in fluoride concentration in the feed water. It can be seen from Table 4 that increased amount of adsorbent bed remained unused when the flow rate was high since at higher flow rates the fluoride solution left the column early.

3.3.2 Column Performance Indicators

The performances of continuous column systems are predicted by the number of bed volumes (BV) treated before the breakthrough point and the adsorbent exhaustion rate (AER) (Malkoc et al. 2006; Senthil Kumar et al. 2010). The number of bed volumes BV is calculated by Eq. (9):

$$BV = \frac{V}{V_{bed}} \tag{9}$$

where V is the volume of water treated and V_{bed} is the volume of the bed. Higher number of bed volumes prior to the breakpoint depicts a better adsorption in the column system. The AER is an indicator of the column performance efficiency and the value of the adsorbent exhaustion rate reflects the goodness of the adsorbent bed performance and is estimated using Eq. (10):

$$AER = \frac{M}{V} \tag{10}$$

where M is the mass of the M-i-HAPa adsorbent pellets (g) and V is the volume treated (L). The

Table 5 Column performance indicators at different operating conditions

Parameters	Z (cm)			F (L/h)			C ₀ (mg/L)		Particle size (mm)		
	5	10	30	1	1.5	2	5	10	<1	1–1.5	1.5–2
Processed BVs	15.30	17.85	22.1	22.1	15.30	8.5	27.21	22.1	23.8	22.1	13.6
AER (g/L)	9.33	7.71	6.15	6.15	8.88	16	5	6.15	5.71	6.15	10

calculated values of BV and AER are given in Table 5. It is noted that the number of bed volumes processed before the breakpoint increased from 15.3 to 22.1 as the bed height increased from 5 cm to 30 cm. The number of bed volumes decreased from 22.1 to 8.5 as the flow rate increased from 1 to 2 L/h. The bed volumes decreased from 27.21 to 22.1 as the initial fluoride concentration varied from 5 to 10 mg/L. Similarly, they decreased from 23.8 to 13.6 as the particle size increased from 1 mm size to 1.5–2 mm sized particles. The adsorbent exhaustion rate was faster at higher flow rates, low bed heights, larger particle sizes and higher fluoride concentrations as expected.

3.4 Adsorbent Regeneration

Regeneration studies provide an insight about the mechanism of adsorption as well as the stability of the adsorbent before further use. The mechanism of sorption of fluoride on adsorbents is either chemical, physical or ion exchange or a combination. Physical adsorption would mean that the fluoride ions are loosely bound to the adsorbent surface and can easily be desorbed. But, if the nature of adsorption is chemical or ion exchange or both, then strong acidic or alkaline solutions need to be used for regeneration. Thus, desorption behavior helps in confirming the mechanism of adsorption. M-i-HAPa pellets saturated with fluoride were washed with double distilled water and only 2% desorption was observed.

After M-i-HAPa pellets were exhausted using 10 mg/L fluoride solution at 1 L/h, they were regenerated using 0.1 M NaOH solution in an upflow mode at a flow rate of 1 L/h for 5 h. Regeneration studies have already been reported in our earlier studies on M-i-HAPa (Mondal et al. 2016) in which four different solutions of sodium hydroxide, sulfuric acid, hydrochloric acid, and potassium hydroxide were tested for regeneration, and it was observed that about 91% regeneration was achieved with 0.1 M NaOH. The flow rate was maintained at 1 L/h, so as to use minimum eluent solution to remove the fluoride ions from the adsorbent bed. For verifying the performance stability of the M-i-HAPa pellets column, four cycles of adsorption and regeneration process were conducted. The volume of eluent collected versus the amount of fluoride desorbed showed that major amount of fluoride, i.e., approx. 80%, was desorbed in the first 1 h and the remaining 20% of fluoride was collected in the next 4 h with a total of 5 L of NaOH solution used, as shown in Fig. 9a. The regenerated adsorbent was further utilized again in the column system for defluoridation and the adsorption capacity was observed to be reduced from 1.01 mg/g to 0.765 mg/g in the second cycle. The capacity was further reduced to 0.4 mg/g in the third cycle and to a very low capacity of only 0.11 mg/g in the fourth cycle. After the adsorbent pellets were subjected to three elution-retention

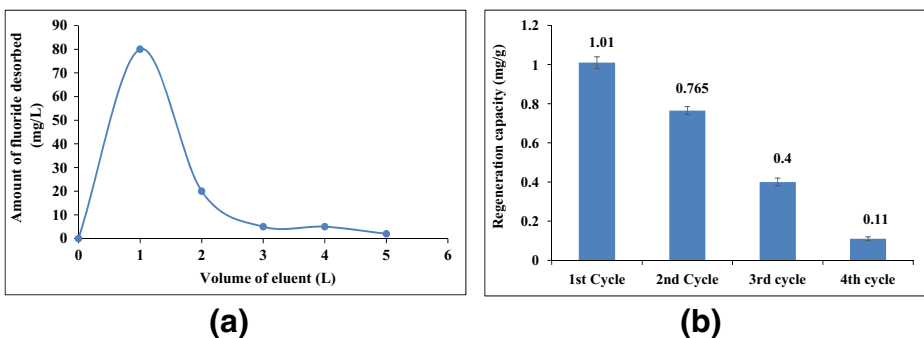


Fig. 9 Desorption-Regeneration Process (a) Desorption of fluoride from M-i-HAPa pellets (b) Regeneration capacity

cycles, their capacity to adsorb fluoride diminished significantly and became unfit for reuse, as shown in Fig. 9b. Tor et al. (2009) found that the adsorbent granular red mud (GRM) could be regenerated up to four cycles while Ghorai and Pant (2005) observed that activated alumina adsorbent could be regenerated up to five cycles. This indicates that for complete use of the synthesized pellets, regeneration is required after every defluoridation cycle. The higher percentage of desorption signify an ion exchange mechanism for adsorption process. Regeneration of M-i-HAPa pellets through alkaline solution supported the fact that adsorption mechanism is chemical in nature.

3.5 Quality Assessment of Treated Water and Studies with Field Water Samples

The physico-chemical properties of treated water were assessed after running the experimental M-i-HAPa column system with fluoridated water having a concentration of 10 mg/L at a flow rate of 1 L/h and bed height of 30 cm. The treated water was collected for 13 h up to the breakthrough point and the water quality parameters were determined which are presented in Fig. 10. The fluoride outlet concentration was 0.9 mg/L and the pH of the treated water was found to be 7.5. The TDS, total hardness, alkalinity in treated water were 230, 118, 185 mg/L, respectively, while the residual concentration of calcium and magnesium were 23 and 23 mg/L, respectively. It is apparent from Fig. 10 that all the physico-chemical parameters were under the permissible limit according to Indian drinking water (BIS 2012) as well as WHO (2011) standards.

The state of Rajasthan, India, is a classic case of falling water tables and increasing incidence of fluoride in water. The state has extreme climatic and geographical conditions with low water resources. Therefore, for conducting field studies, regions in the four districts viz. Sikar, Jodhpur, Jaipur and Dausa of Rajasthan were chosen, where 20 to 40% of villages have been reported to be affected with excess fluoride (concentration range 1 to 12 mg/L) in water (Yadav et al. 2009). Water quality parameters such as pH, EC, TDS, salinity, alkalinity, total hardness, turbidity, Cl^- , Ca^{2+} , Mg^{2+} and F^- for different places are enlisted in Table 6. It is evident that the villages with lower fluoride concentration have higher concentrations of calcium and vice versa. This is attributed to the fact that the presence of higher concentrations of calcium ions decreased the solubility of fluoride as calcium ions bind with fluoride ions to form CaF_2 . High alkalinity in groundwater favored higher fluoride concentration in water when the pH varied between 6.8 to 8.5. The turbidity value was observed to be very low for all the field water samples. Among the samples collected, water collected from Kanteva village

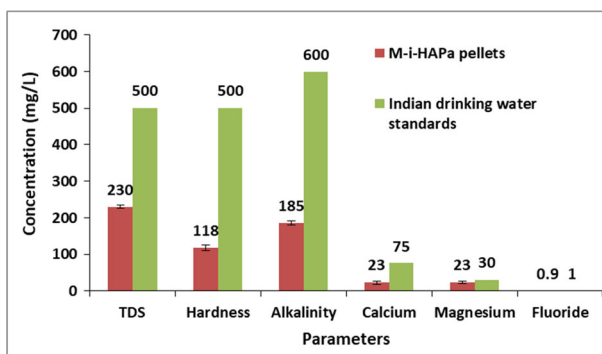


Fig. 10 Water quality parameters examined after column studies with M-i-HAPa pellets (Inlet F conc. 10 mg/L, flow rate 1 L/h, bed height 30 cm)

Table 6 Characteristics of groundwater samples from various districts of Rajasthan, India

Parameters	District: Sikar		District: Jodhpur		District: Jaipur		District: Dausa	
	Kanteva village	Bhooma chota village	Basni	Ratanada	Pratap nagar	Malaviya Nagar	Bandikui	Bandikui
F ⁻ (mg/L)	2.76	5.22	12.6	0.685	0.460	0.8	2.5	2.5
Ca ⁺⁺ (mg/L)	69	46	58	256	432	297	80	80
Mg ⁺⁺ (mg/L)	17	23	57	62	29	28	66	66
Hardness (mg/L)	139	142	295	512	555	415	352	352
Alkalinity (mg/L)	300	395	200	197	200	84	220	220
Turbidity (NTU)	0	0.11	0	0	0.26	0	0.41	0.41
pH	8.13	8.4	8.08	6.8	7.89	8.06	8.5	8.5
Cl ⁻ (mg/L)	165	310	1520	500	117	248	220	220
TDS (mg/L)	770	1419	3752	678	251	375	1271	1271
Conductivity (µS/cm)	1572	2882	7660	1389	512	754	2545	2545
Salinity (psu)	0.874	1.654	4.685	0.798	0.274	0.431	2.34	2.34

and Bhoomchota village in Sikar district, Basni village in Jodhpur district and Bandikui in Dausa district had fluoride concentrations higher than the permissible limit of 1.0 mg/L.

Defluoridation experiments were carried out through column studies for the field water from Basni village, Jodhpur district which had the highest fluoride concentration among the field samples (i.e., 12.6 mg/L). The fluoride concentration of the treated water using M-i-HAPa pellets was found to be 0.9 mg/L which is under the permissible limit of 1 mg/L. Moreover, after treating the Basni village water sample with M-i-HAPa pellets, the TDS, total hardness and alkalinity were observed to be 255, 160 and 200 mg/L, respectively. The concentration of calcium and magnesium in the treated sample were 23 and 25 mg/L, respectively, and the pH of water after treatment was 7.82. The suitability of M-i-HAPa pellets as a potent adsorbent is clearly depicted from the quality of water obtained.

3.6 Domestic Defluoridation Unit (DDU)

Considering the domestic needs of people, a domestic defluoridation unit was designed assuming that approximately 5 L of water will fulfill the daily requirement for cooking and drinking per person. In this study, a domestic defluoridation unit based on M-i-HAPa pellets as the adsorbent was designed as shown in Fig. 11. The performance

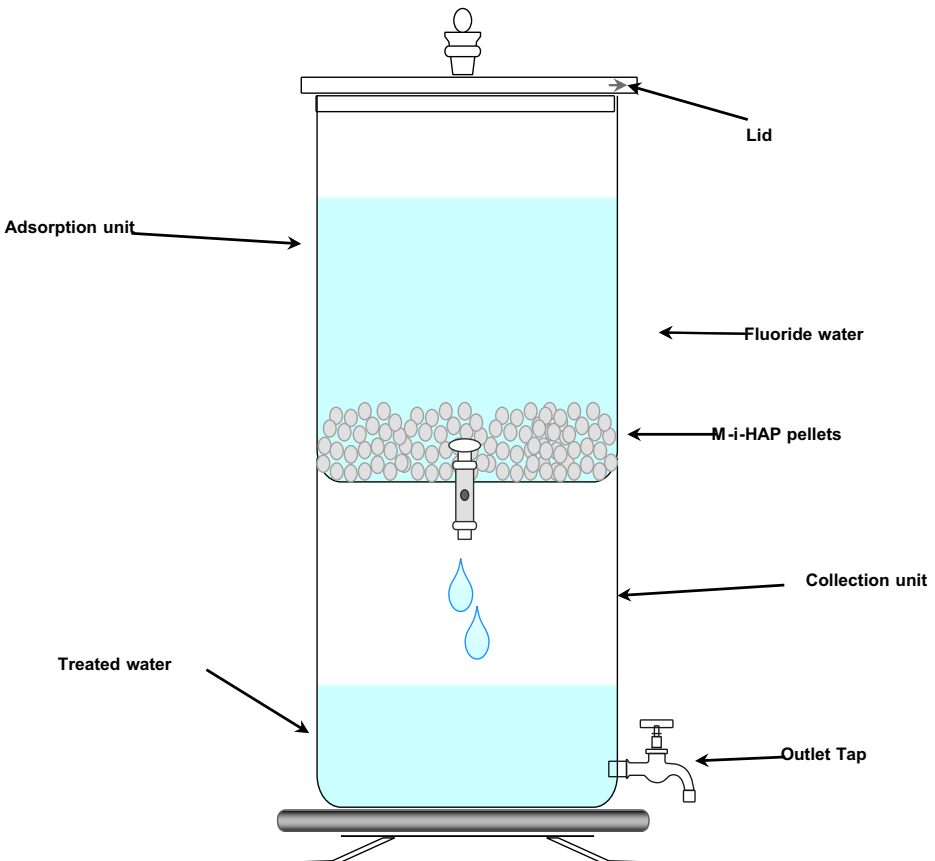


Fig. 11 Domestic defluoridation unit

Table 7 Characteristics of activated alumina and M-i-HAPa pellets

S.no.	Characteristics	Activated alumina (Chauhan et al. 2007)	M-i-HAPa pellets (Present study)
1	Particle form	Spheres	Spheres
2	Particle size (mm)	0.4–1.2	1–1.5
3	Surface area (m ² /g)	310	21.22
4	Pore volume (cm ³ /g)	0.41	0.096
5	Fluoride uptake capacity (mg/g)	1.788	1.16

of the DDU designed for M-i-HAPa pellets was compared with that of activated alumina based DDU reported by Chauhan et al. (2007) and by Venkobachar et al. (1997). The characteristics of activated alumina used in their study and corresponding characteristics of M-i-HAPa pellets are listed in Table 7. The fluoride uptake capacity was reported to be 1.788 mg/g by Chauhan et al. (2007) and 1.83 mg/g by Venkobachar et al. (1997) for activated alumina, when 3 kg of activated alumina was used in the DDU for treating the fluoride concentration in water from 10 ± 0.5 mg/L to fluoride concentration below 1 mg/L. The water flow of the slot opening between the two chambers in the DDU was as reported at 9 to 10 L for the activated alumina DDU unit. It was reported that using 3 kg of activated alumina, the volume of water treated (for $F^- \leq 1.5$ mg/L) was 550 L. The domestic defluoridation unit had activated alumina bed dimensions: 22 cm diameter and 23 cm height. Further, the exhausted activated alumina was regenerated using 1% NaOH followed with acid treatment and the adsorbent was reused for five cycles (Chauhan et al. 2007).

In this study, the capacity of M-i-HAPa adsorbent was found to be 1.16 mg/g for an initial fluoride concentration of 10 mg/L. Therefore, approximately 348 L of 10 mg/L fluoride water could be treated with 3 kg of the adsorbent in the DDU. The slot opening between the adsorption and collection chamber was maintained at a flow rate of 5 to 6 L/h. The dimensions for each chamber of the DDU was 30 cm height and 25/23 (top/bottom) diameter. The fluoride solution and adsorbent were given a residence time of 3 h (equilibrium time) before collecting the treated water. The field water sample from Basni village which had fluoride concentration of 12.6 mg/L (highest among the field data obtained) was treated in the DDU and the fluoride uptake capacity was observed at 1.086 mg/g of M-i-HAPa adsorbent and approximately 259 L of water was treated with 3 kg of adsorbent. In this study, M-i-HAPa adsorbent was regenerated using 0.1 M NaOH for 90 min, and thereafter, the adsorbent was dried at 95 °C for 60 min. Ninety one percent regeneration was achieved and after using for five consequent cycles the removal efficiency was minimal and the adsorbent was unfit for further use.

On comparing the values of fluoride uptake capacity for AA and M-i-HAPa (1788 and 1160 mg/kg adsorbent, respectively), it can be seen that AA had slightly higher fluoride uptake capacity. However, usage of AA defluoridation units may lead to leaching of aluminum in ionic and complex form of alumino-fluoro complexes (George et al. 2010). The residual aluminum in treated water, if consumed, can cause severe health issues. On the other hand, the M-i-HAPa adsorbent consists of only calcium and magnesium compounds, which are completely safe to use for defluoridation of drinking water (as leaching of Ca^{2+} and Mg^{2+} are within the permissible

limits). The spent adsorbent, which is rich in fluoride, can be a suitable raw material for making cement, refractory bricks or for direct use in road construction purposes.

4 Conclusions

The following conclusions are drawn from the present study:

- The magnesium incorporated Hydroxyapatite M-i-HAPa, synthesized via the chemical precipitation route and pelletized using PVA binder to form spherical pellets, was found to be an effective defluoridation agent in column adsorption system with an adsorption capacity of 1.46 mg/g for feed fluoride concentration of 10 mg/L, flow rate 1 L/h and bed height 30 cm. Characterization studies revealed that with fluoride adsorption, formation of hydroxyfluorapatite, fluorapatite and magnesium fluoride occurred on the adsorbent surface which was regenerated effectively using 0.1 M NaOH solution. The specific surface area of M-i-HAPa pellets was found to be 21.22 m²/g while the pore volume and pore diameter was observed to be 0.096 cm³/g and 181.59 Å, respectively.
- Adsorption column dynamics was also studied through simulated and experimental breakthrough curves with varying flow rates and particles sizes. On analyzing the breakthrough curves under different process conditions, it was observed that bed height of 30 cm with 1–1.5 mm pellets of spherical particle sizes and flow rate of 1 L/h and feed fluoride concentration of 10 mg/L were optimum for efficient column performance. The experimental breakthrough curves obtained by varying flow rate and size of particles were compared for convergence with simulated curves obtained by the adsorption simulator “ADSORB” developed in MATLAB software.
- The performance of the column system was evaluated in terms of number of bed volumes and adsorbent exhaustion rate. It was noticed for 30 cm bed height that 22.1 bed volumes can be processed and the AER for the same was 6.15 g/L.
- Regeneration studies showed that the pellets were stable for repeated use up to four times. Desorption experiments also confirmed the ion exchange mechanism dominating the process of adsorption. The physicochemical parameters of treated water were found to be as per the standards set by WHO and BIS for drinking source; moreover, the treated water was only rich in calcium and magnesium which is suitable for alleviating fluorosis in people caused by the prolonged consumption of fluoride in drinking water. Thus, this study affirms the practical feasibility of using M-i-HAPa pellets for effective defluoridation via column studies.

Acknowledgements This work is part of original research towards the fulfillment of doctoral thesis work conducted at Malaviya National Institute of Technology (MNIT) Jaipur, India. The authors are thankful for the infrastructure and characterization facilities available at Materials Research Centre, MNIT Jaipur needed for this paper. Dr. Suja George is thankful to DST Rajasthan for providing funding to setup few facilities useful for conducting the research presented in this work.

References

APHA/AWWA/WEF (2012) Standard methods for the examination of water and wastewater. Standard Methods, 541. ISBN 9780875532356

- Ayoob S, Gupta AK, Bhakat PB, Bhat VT (2008) Investigations on the kinetics and mechanisms of sorptive removal of fluoride from water using alumina cement granules. *Chem Eng J* 140(1–3):6–14. <https://doi.org/10.1016/j.cej.2007.08.029>
- Bhaumik R, Mondal NK (2015) Adsorption of fluoride from aqueous solution by a new low-cost adsorbent: thermally and chemically activated coconut fibre dust. *Clean Techn Environ Policy* 17(8):2157–2172. <https://doi.org/10.1007/s10098-015-0937-6>
- BIS (2012) Indian standard: drinking water-specification (second revision), IS 10500. www.bis.org.in/other/DrinWatI10500.pdf
- Chabert F, Dunstan DE, Franks GV (2008) Cross-linked polyvinyl alcohol as a binder for gelcasting and green machining. *J Am Ceram Soc* 91(10):3138–3146. <https://doi.org/10.1111/j.1551-2916.2008.02534.x>
- Chauhan VS, Dwivedi PK, Iyengar L (2007) Investigations on activated alumina based domestic defluoridation units. *J Hazard Mater* 139:103–107. <https://doi.org/10.1016/j.jhazmat.2006.06.014>
- Chen N, Feng C, Li M (2014) Fluoride removal on Fe–Al-impregnated granular ceramic adsorbent from aqueous solution. *Clean Techn Environ Policy* 16(3):609–617. <https://doi.org/10.1007/S10098-013-0659-6>
- Fan X, Parker DJ, Smith MD (2003) Adsorption kinetics of fluoride on low cost materials. *Water Res* 37(20):4929–4937. <https://doi.org/10.1016/j.watres.2003.08.014>
- George S, Pandit P, Gupta AB, Agarwal M (2009) Modeling and simulation studies for aluminium-fluoride interactions in Nalgonda defluoridation process. *Chem Prod Process Model* 4. <https://doi.org/10.2202/1934-2659.1367>
- George S, Pandit P, Gupta AB (2010) Residual aluminium in water defluoridated using activated alumina adsorption-modeling and simulation studies. *Water Res* 44(10):3055–3064. <https://doi.org/10.1016/j.watres.2010.02.028>
- Ghorai S, Pant KK (2005) Equilibrium, kinetics and breakthrough studies for adsorption of fluoride on activated alumina. *Sep Purif Technol* 42:265–271. <https://doi.org/10.1016/j.seppur.2004.09.001>
- Ghosh A, Chakrabarti S, Biswas K, Ghosh UC (2015) Column performances on fluoride removal by agglomerated Ce(IV)-Zr(IV) mixed oxide nanoparticles packed fixed-beds. *J Environ Chem Eng* 3(2):653–661. <https://doi.org/10.1016/j.jece.2015.02.001>
- Isiklan N, Sanli O (2005) Separation characteristics of acetic acid-water mixtures by pervaporation using poly(vinyl alcohol) membranes modified with malic acid. *Chem Eng Process Process Intensif* 44(9):1019–1027. <https://doi.org/10.1016/j.cep.2005.01.005>
- Jimenez-Reyes M, Solache-Rios M (2010) Sorption behavior of fluoride ions from aqueous solutions by hydroxyapatite. *J Hazard Mater* 180(1):297–302. <https://doi.org/10.1016/j.jhazmat.2010.04.030>
- Kamble SP, Dixit P, Rayalu S, Labhsetwar N (2009) Defluoridation of drinking water using chemically modified bentonite clay. *Desalination* 249:687–693. <https://doi.org/10.1016/j.desal.2009.01.031>
- Kundu S, Gupta AK (2005) Analysis and modeling of fixed bed column operations on As(V) removal by adsorption onto iron oxide-coated cement (IOCC). *J Colloid Interface Sci* 290(1):52–60. <https://doi.org/10.1016/j.jcis.2005.04.006>
- Maliyekkal SM, Shukla S, Philip L, Nambi IM (2008) Enhanced fluoride removal from drinking water by magnesia-amended activated alumina granules. *Chem Eng J* 140:183–192. <https://doi.org/10.1016/j.cej.2007.09.049>
- Malkoc E, Nuhoglu Y, Abali Y (2006) Cr(VI) adsorption by waste acorn of *Quercus ithaburensis* in fixed beds: prediction of breakthrough curves. *Chem Eng J* 119(1):61–68. <https://doi.org/10.1016/j.cej.2006.01.019>
- Meenakshi MRC (2006) Fluoride in drinking water and its removal. *J Hazard Mater* 137(1):456–463. <https://doi.org/10.1016/j.jhazmat.2006.02.024>
- Mehta D, Mondal P, George S (2016) Utilization of marble waste powder as a novel adsorbent for removal of fluoride ions from aqueous solution. *J Environ Chem Eng* 4(1):932–942. <https://doi.org/10.1016/j.jece.2015.12.040>
- Mehta D, Mondal P, Saharan VK, George S (2017) Synthesis of hydroxyapatite nanorods for application in water defluoridation and optimization of process variables: advantage of ultrasonication with precipitation method over conventional method. *Ultrason Sonochem* 37:56–70. <https://doi.org/10.1016/j.ultrsonch.2016.12.035>
- Mehta D, Mondal P, Saharan VK, George S (2018) In-vitro synthesis of marble apatite as a novel adsorbent for removal of fluoride ions from ground water: an ultrasonic approach. *Ultrasonics Sonochemistry* 40, part a: 664–674. <https://doi.org/10.1016/j.ultrsonch.2017.08.015>
- Mondal P, George S (2015a) A review on adsorbents used for defluoridation of drinking water. *Rev Environ Sci Biotechnol* 14(2):195–210. <https://doi.org/10.1007/s11157-014-9356-0>
- Mondal P, George S (2015b) Removal of fluoride from drinking water using novel adsorbent magnesia-hydroxyapatite. *Water Air Soil Pollut* 226:241. <https://doi.org/10.1007/s11270-015-2515-2>
- Mondal P, Mehta D, George S (2016) Defluoridation studies with synthesized magnesium-incorporated hydroxyapatite and parameter optimization using response surface methodology. *Desalin Water Treat* 57(56):27294–27313. <https://doi.org/10.1080/19443994.2016.1167628>

- Percival M (1999) Bone health and osteoporosis. *Appl Nutr Sci Report* 5:1–5 <http://www.healingpoints.com/Osteoporosis.PDF>
- Rafique AA, Awan MA, Wasti A, Qazi IA, Arshad M (2012) Removal of fluoride from drinking water using modified immobilized activated alumina. *J Chem.* <https://doi.org/10.1155/2013/386476>
- Sarkar M, Banerjee A, Pramanick PP, Sarkar AR (2006) Use of laterite for the removal of fluoride from contaminated drinking water. *J Colloid Interface Sci* 302:432–441. <https://doi.org/10.1016/j.jcis.2006.07.001>
- Senthil Kumar P, Ramalingam S, Senthamarai C, Niranjana M, Vijayalakshmi P, Sivanesan S (2010) Adsorption of dye from aqueous solution by cashew nut shell: studies on equilibrium isotherm, kinetics and thermodynamics of interactions. *Desalination* 261(1–2):52–60. <https://doi.org/10.1016/j.desal.2010.05.032>
- Thakre D, Rayalu S, Kawade R, Meshram S, Subrt J, Labhsetwar N (2010) Magnesium incorporated bentonite clay for defluoridation of drinking water. *J Hazard Mater* 180:122–130. <https://doi.org/10.1016/j.jhazmat.2010.04.001>
- Tor A, Danaoglu N, Arslan G, Cengeloglu Y (2009) Removal of fluoride from water by using granular red mud: batch and column studies. *J Hazard Mater* 164(1):271–278. <https://doi.org/10.1016/j.jhazmat.2008.08.011>
- Tripathy SS, Raichur AM (2008) Abatement of fluoride from water using manganese dioxide-coated activated alumina. *J Hazard Mater* 153(3):1043–1051. <https://doi.org/10.1016/j.jhazmat.2007.09.100>
- Venkobachar C, Iyengar L, Mudgal AK (1997) Household defluoridation of drinking water using activated alumina. 2nd International Workshop on Fluorosis Prevention and Defluoridation of Water, 138–145. <http://www.de-fluoride.net/2ndproceedings/138-145.pdf>
- WHO (2011) Guidelines for drinking-water quality, (fourth edition), Geneva: World Health Organization. http://whqlibdoc.who.int/publications/2011/9789241548151_eng.pdf
- Wilson DI, Rough SL (2007) Chapter 3: extrusion-spheronisation. *Handb Powder Technol* 11:189–217. [https://doi.org/10.1016/S0167-3785\(07\)80038-8](https://doi.org/10.1016/S0167-3785(07)80038-8)
- Yadav AK, Khan P, Saxena U (2009) Geochemical observation of fluoride in ground water of Tonk (Rajasthan), *Rasayan J. Chem* 2(4):994–1000 www.rasayanjournal.co.in/vol-2/issue-4/36.pdf
- Young CR, Koleng JJ, McGinity JW (2002) Production of spherical pellets by a hot-melt extrusion and spheronization process. *Int J Pharm* 242(1–2):87–92. [https://doi.org/10.1016/S0378-5173\(02\)00152-7](https://doi.org/10.1016/S0378-5173(02)00152-7)
- Zhao B, Zhang Y, Dou X, Wu X, Yang M (2012) Granulation of Fe-Al-Ce trimetal hydroxide as a fluoride adsorbent using the extrusion method. *Chem Eng J* 185–186:211–218. <https://doi.org/10.1016/j.cej.2012.01.085>